THE ASTROPHYSICAL JOURNAL, 686: L45–L48, 2008 October 10

EVIDENCE FOR A CURRENT SHEET ABOVE A SUNSPOT UMBRA

A. TRITSCHLER,[1] H. UITENBROEK,[1] AND K. REARDON[1,2]

Received 2008 January 28; accepted 2008 August 26; published 2008 September 11

ABSTRACT

We present observational evidence for the existence of a current sheet in the chromosphere above a sunspot umbra based on high angular resolution two-dimensional spectroscopic observations in the Ca II 854.21 nm line. In the core of this line we observe a very stable bright ribbon-like structure separating magnetic field configurations that connect to different parts of the active region. We make plausible that the structure is a string of sheets carrying vertical currents that result from dissipation when the different parts of the active region are moved around in the photosphere. To our knowledge this is the first direct observation of the heating caused by the dissipation in such a current sheet in the chromosphere.

Subject headings: magnetic fields — Sun: chromosphere — sunspots

Online material: color figure

1. INTRODUCTION

The dissipation of magnetic energy by current sheets is one of several possible mechanisms that have been suggested to heat the solar chromosphere and corona (see Parker 1983a, 1983b). In addition, the formation of current sheets may contribute to the powering of solar flares (e.g., Priest 1987; Ji et al. 2004). According to Parker (1983a) current sheets form spontaneously when the foot points of magnetic loops are subjected to complex differential motions in the photosphere. Given the non-negligible plasma β (the ratio of gas over magnetic pressure), the plasma cannot adjust to a new force-free equilibrium and instead gives rise to the formation of current sheets.

Barring direct observational evidence, the existence of these current sheets has been indirectly deduced from vector magnetograms as for instance performed by Solanki et al. (2003). Using spectropolarimetric observations in the He I 1083.0 nm triplet these authors found indication for the presence of a current sheet between two areas of opposite polarity in an active region. Socas-Navarro (2005a, 2005b) instead used the non-LTE inversion of a spectropolarimetric map of a sunspot in the Ca II 849.8 nm and 854.2 nm lines to reconstruct a three-dimensional map of the temperature, velocity, and magnetic field vector from the photosphere up into the chromosphere. The derived current density indicates that the strongest currents in the active region are concentrated in filamentary structures in horizontal cross sections, and sheets in three dimensions. These structures are not aligned with the magnetic field, implying that the currents result from a forcing of the magnetic field. However, at the spatial resolution achieved with these observations only a weak positive correlation is found between the computed current density and the temperature. A slightly better correlation was observed between current density and positive temperature gradients between 400 and 1400 km, indicating the presence of heating in that height range.

In this Letter we present evidence of the presence of electric current dissipation in an active region from observations that are complimentary to the previous ones. Because of the very high spatial resolution in our observations we are able to directly observe the heating of the chromospheric plasma by steady current dissipation through the brightening it causes in and close to the core of the Ca II 854.2 nm line at wavelengths which form between 400–800 km geometrical height.

2. OBSERVATIONS AND DATA ANALYSIS

Observations have been carried out on 2006 August 24 at the Dunn Solar Telescope (DST) of the National Solar Observatory (NSO), Sunspot, New Mexico using the Interferometric BIdimensional Spectrometer (IBIS; Cavallini 2006).[3] IBIS is a dual Fabry-Pérot system in a collimated mount. Real-time seeing correction and image stabilization was accomplished by the high-order adaptive optics system at the DST (Rimmele 2004). We followed the leading sunspot of bipolar NOAA active region 10905 (S08 E36, viewing angle of 36°) for 120 minutes from 15:49 to 17:49 UT during which we obtained 190 scans of the Ca II 854.2 nm, Na I D1, and Fe I 709.04 nm lines. Here we only employ the Ca II line scans, which consist of 41 exposures each, acquired within 10 s taken at non-equidistant wavelength points with an average step width of 2.5 pm. Exposure time and cycle time of each sequence was 20 ms and 37 s, respectively. IBIS was operated in a spatially binned mode with a total field of view of 80″ × 80″, an image scale of 0.165″ pixel^{-1}, and a spectral resolution larger than 200,000 at Ca II 854.2 nm (Reardon & Cavallini 2008). The narrowband prefilter had a full width at half-maximum of 0.5 nm. The broadband channel of IBIS was equipped with an interference filter centered at 721.63 nm with a width of 9.6 nm.

Standard calibration procedures for a collimated configuration encompassed dark subtraction, gain table and blueshift correction, and correction for the influence of the wavelength dependence of the prefilter transmission. Grid targets were used to determine the offset, rotation and image scale differences between the narrowband filtergrams and the simultaneous broadband images. The broadband data were employed to correct for image shifts, image distortions (destretch), and transparency fluctuations that might have taken place during the scanning of the line.

After the calibration we used the scanned profiles of the Ca II

[1] National Solar Observatory/Sacramento Peak, P.O. Box 62, Sunspot, NM 88349; ali@nso.edu, huitenbroek@nso.edu. The NSO is operated by the Association of Universities for Research in Astronomy, Inc. (AURA), for the National Science Foundation.

[2] INAF–Observatorio Astrofisico di Arcetri, I-50125 Firenze, Italy; kreardon@arcetri.astro.it.

[3] IBIS has been built by INAF/Osservatorio Astrofisico di Arcetri with contributions from the Universities of Firenze and Roma "Tor Vergata," the NSO, and the Italian Ministries of Research (MIUR) and Foreign Affairs (MAE).

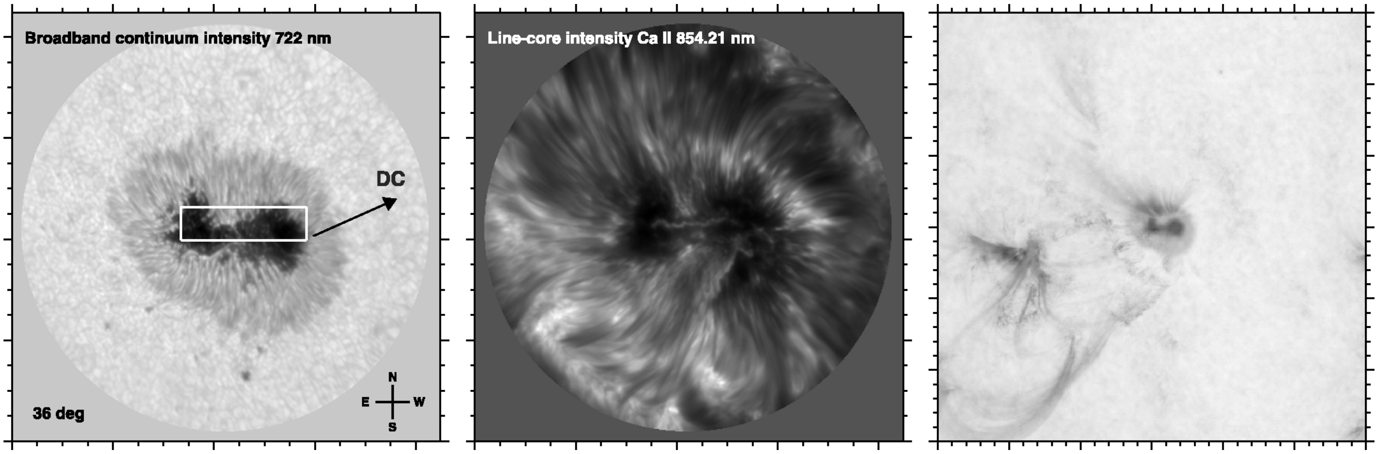

FIG. 1.—Broadband continuum intensity at 722 nm (*left*) and line-core intensity of the Ca II 854.21 nm line (*middle*) of AR 10905 (S08 E36) at 16:35 UT. The arrow points toward disk center (DC). Minor tick marks correspond to 5″. *Right*: Superposition of a MDI continuum intensity filtergram observed at 17:52 UT on 2006 August 24, and a co-aligned, false-color, negative 171 Å image obtained with *TRACE* at 03:48 UT on the same day indicating the transition region morphology of AR 10905 at about 1×10^6 K. One minor tick mark corresponds to 10″. The white rectangle indicates the zoom-in FOV used in Fig. 3. [*See the electronic edition of the Journal for a color version of this figure.*]

854.2 nm line at each spatial pixel to extract the line-core intensity and calculate line-of-sight (LOS) velocities from Doppler shifts utilizing a Fourier phase method (Schmidt et al. 1999). Our wavelength scale is a relative wavelength scale using the area outside the sunspot (determined from the broadband continuum intensity) as a reference. In contrast to the astrophysical convention we assign a negative sign to redshifts (dark, away from the observer) and a positive sign to blueshifts (bright, toward the observer).

In addition, we compare our observations with cotemporal photospheric magnetograms obtained with the Michelson Doppler Interferometer (MDI; Scherrer et al. 1995) on board the *SOHO* satellite, and UV 171 Å observations obtained with the *Transition Region and Coronal Explorer* (*TRACE*; Handy et al. 1999).

3. RESULTS

The line-core intensity reveals diverse and ubiquitous fine structure emanating from the sunspot and its penumbra. High- and low-lying loop structures in the form of dark fibrils connect the sunspot to the surrounding network, pores, and trailing polarity. We note a very conspicuous ribbon-like structure located inside the sunspot umbra mostly oriented in east-west direction with curved endings to both sides (see Fig. 1, *middle*) and a bead-like substructure. The ribbon is not related to the numerous umbral dots observable in the photosphere (see Fig. 1, *left*) which is corroborated by Figure 3 where we show a close-up of the broadband intensity image (*top*) and the time averaged line-core intensity (*middle*). Moreover, the ribbon is not apparent in *TRACE* data reflecting transition region conditions (see Fig. 1, *right*). It is limited to layers defined by the formation height of central parts of the Ca II 854.21 nm line as is demonstrated in Figure 2. We interpret the ribbon as the radiative signature of dissipation in a current sheet as we make plausible below.

The temporal average of the line-core intensity of the current sheet (Fig. 3, *middle*) supports the impression that during the 120 minute sequence the location of the current sheet remains

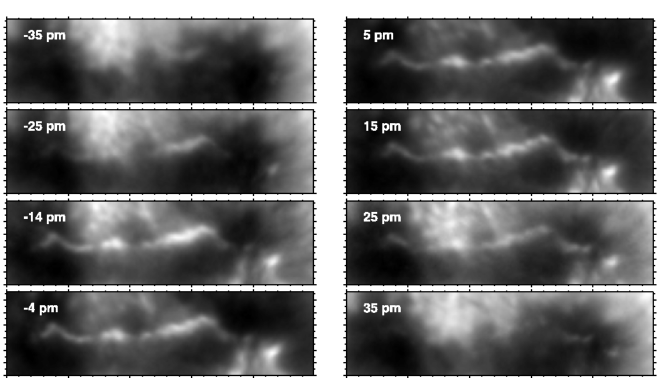

FIG. 2.—Selected wavelengths through the Ca II 854.21 nm line showing the central part of the umbra where the ribbon-like structure appears as marked by the white rectangle in Fig. 1. Indicated wavelength positions are given with respect to the line-core position of the line profiles averaged over areas outside the sunspot. Major tick marks in the *x*- and *y*-directions correspond to 5″ and 1″, respectively.

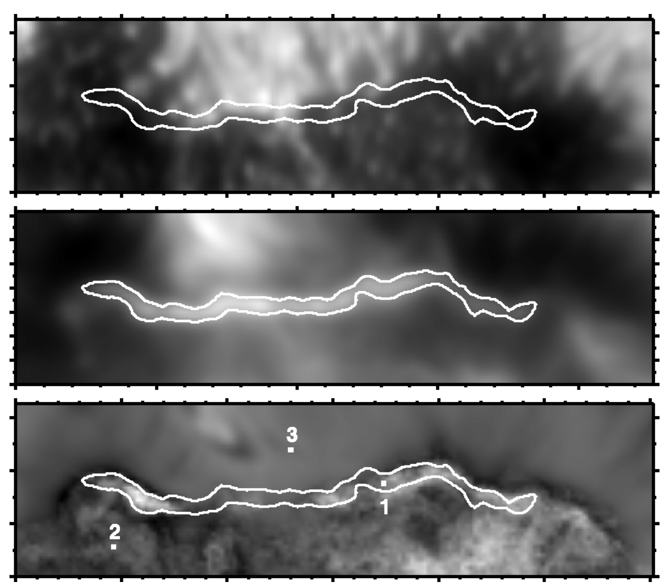

FIG. 3.—Individual broadband continuum intensity image (*top*) and line-core intensity image (*middle*) averaged over the 120 minute observing time. *Bottom*: Average LOS velocity as derived from the Fourier technique (see text). Velocities are in the range −2.8 to 2.6 km s^{-1}. Major tick marks as in Fig. 2. Contour lines outline the location of the ribbon-like structure.

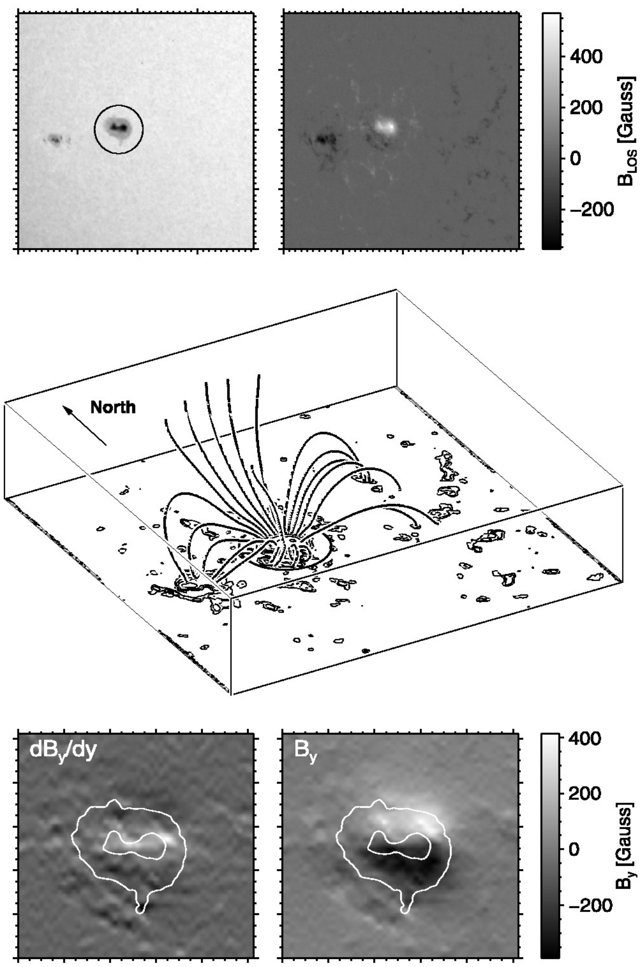

FIG. 4.—*Top*: MDI continuum intensity (*left*) and line-of-sight magnetic flux density (*right*) of AR 10905 observed on 2006 August 24 at 17:35 UT. Major tick marks correspond to 100″. The circle overlaid on the intensity image indicates the FOV of IBIS. *Middle*: Magnetic topology of AR 10905 as derived from the MDI magnetic flux density (see text). *Bottom*: Horizontal component of the extrapolated field in the north-south direction (*right*) and its derivative. Major tick marks correspond to 20″. Contour lines outline the visible boundary of the sunspot penumbra and umbra as derived from the MDI continuum intensity.

virtually unchanged notwithstanding its dynamic environment. We observe umbral oscillations and flashes with periods of 3 minutes progressing into penumbral waves. The dark chromospheric filaments in the line-core intensity carry inward flows of up to ∼10 km s^{-1} (inverse Evershed flow). The current sheet does not seem to be significantly disturbed by any of these processes and does not itself show up in a mean LOS Dopplergram (see Fig. 3, *bottom*). However, the mean Dopplergram indicates that the current sheet is spatially located close to a steep horizontal gradient in the LOS velocity. This gradient and the current sheet seem to separate two different loop systems that emanate from the sunspot (umbra): bright low-lying loops directed toward the southeast, and darker, more vertical loops directed toward the north. These loop systems are apparent from both the line-core intensity (Fig. 1, *middle*) and the *TRACE* image (Fig. 1, *right*). We argue that the very different inclinations of these loop systems and the shear between them results in the current sheet.

To model the magnetic field configuration above the active region (given the lack of spectropolarimetric observations) we

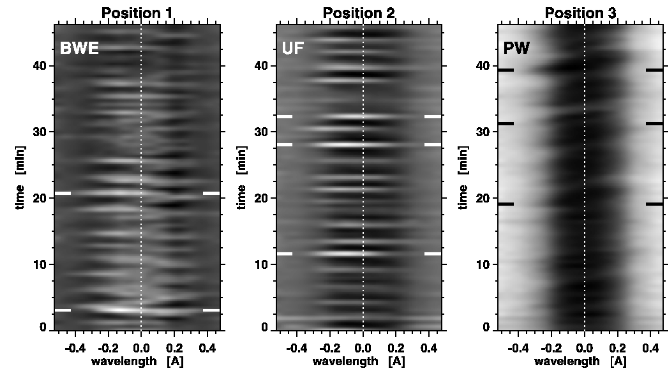

FIG. 5.—Spectral-time slices for different positions in the sunspot as indicated in Fig. 3 (*bottom*). BWE: Blue-wing emission. UF: Umbral flashes. PW: Propagating waves.

apply a potential field extrapolation technique to the photospheric boundary conditions as given by a quasi-simultaneous MDI magnetogram (see Fig. 4, *right*). This field extrapolation cannot reproduce the true field configuration; however, it should give a reasonable description of the large-scale loop structure. The result of this effort is shown in Figure 4 (*middle*) supporting the idea that two loop structures with very different geometry, separated by the current sheet, emanate from the sunspot. The field extrapolation recovers shallow field lines that connect to the immediate surroundings to the southeast and longer field lines connecting to regions farther away to the north outside our FOV. Given the location of the current sheet we consider these two to be the relevant loops systems. The field lines that connect to the trailing polarity of the active region toward the east (also observed in the line-core intensity in Fig. 1, *middle*) are in a direction parallel to the axis of the current sheet and therefore cannot contribute to the dissipation in it.

Further evidence of a strong gradient in field line linkage is seen in the colocation between the bright ribbon, and a strong gradient in the horizontal component of the extrapolated potential field B_y (*right*) and the large values of its derivative dB_y/dy with respect to the north-south direction (*left*) shown in the bottom panels of Figure 4. The large values of dB_y/dy give rise to a quasi-separatrix layer (QSL; see Priest & Démoulin 1995; Demoulin et al. 1996), which does not provide direct evidence for a current sheet, but identifies a region that is susceptible to shear and the formation of a tangential discontinuity in the field.

The line profiles in and around the current sheet feature a variety of different shapes on top of an overall participation in the (spatially coherent) 3 minute umbral oscillations. To demonstrate this we select several spatial positions as indicated in Figure 3 (*bottom*) and display their corresponding stacked spectral profiles for the first 46 minutes in Figure 5. Comparing the behavior at the different positions we note that the spectral profiles associated with the two loop systems are inherently different. Since we have spectral and temporal information in each pixel in our two-dimensional FOV, we verified based on spacetime slices through each of the marked positions (not shown here) that in the more vertical loops (position 3) we mostly have propagating waves (PW) (e.g., Bloomfield et al. 2007). The low-lying loop system and the current sheet (positions 1 and 2) are dominated by umbral flashes (UF). In addition, the latter positions exhibit episodic events that correspond to exceptionally strong blue wing brightenings (BWE), as for instance appear at the times marked with the horizontal bars in the slice for position 1. It is well known that Ca II K spectra associated with K_{2v} grains develop a redshifted line core in combination with strong brightening of the K_{2v} emission peak and that this pattern is evidence of the passing of an acoustic shock wave (e.g., Carlsson & Stein 1997). A similar pattern may occur in the wing of the Ca II 854.2 nm line when a strong shock crosses the line core forming region (Uitenbroek et al. 2006). In this case the blue wing develops an emission reversal that corresponds to the enhanced K_{2v} in the K line. It is not clear whether episodes of the strong blue-wing emission marked in the position 1 time slice are extreme cases of this pattern, or whether a different physical mechanism is at play. In some cases we found the strong wing brightening to be part of the local pattern by looking at the spectra of neighboring pixels. In these cases the extreme values observed at position 1 were the culmination of the blue wing emission and red shift in the surrounding area. In other cases we could not find such a connection and suggest the contribution of a different more localized physical mechanism. One alternative is that the strong reversals correspond to intermittent fast reconnection events (compare with Katsukawa et al. 2007; Jurcak & Katsukawa 2008 in the context of the penumbra) that adds its signature to the general oscillatory pattern.

4. DISCUSSION AND CONCLUSIONS

We have described novel spectroscopic sunspot observations obtained in the Ca II 854.2 nm line that unveil the presence of a conspicuous ribbon-like structure in the sunspot's umbra which has not been observed before. We conjecture that the ribbon is the visual consequence of dissipation of magnetic energy by a current sheet induced by the presence of two loop systems emerging from the sunspot with very different field geometry.

Both loop structures connect to different parts of the active region and the relevant differential footpoint motion introduces a shear between the more shallow and more vertical magnetic field bundle. Since the field cannot relax to force-free equilibrium this configuration forces the tangential component of the magnetic field flux density to be discontinuous at the interface of the two loop structures. The resulting current is directed perpendicular to the normal of the interface and normal to the discontinuity in the tangential component of the magnetic flux density. Its strength is proportional to the magnitude of the jump. Since the discontinuity appears in the horizontal field component, the current has to be vertical.

The intensity in the Ca II 854.2 nm line comes from a broad range of heights in the solar atmosphere, ranging from the photosphere in the wings to the chromosphere in the central part of the line (Cauzzi et al. 2008). We find that the ribbon's presence in height is limited to a range which corresponds to the formation extent of the line core. The dissipation of the current, therefore, seems to occur only in the higher layers of the active region, where it causes higher temperatures and enhanced excitation in the line. To characterize the vertical extent of the current sheet more quantitatively we estimate the formation height of the intensity in the line at those wavelengths where the ribbon shows enhanced brightness by computing the line intensity contribution function (Uitenbroek 2006) based on a sunspot model (Socas-Navarro et al. 2000). Since the current sheet is visible all the way through the central part of the line, we cannot determine an upper boundary beyond the formation height of the very core of the line. In this way we find 400 km for the lower bound of the heating associated with the current sheet, and 800 km for its upper bound. These heights agree very well with the estimates of Goodman (2004) who finds that the chromosphere is efficiently heated by current dissipation of the current component perpendicular to the magnetic field (the Pedersen current) only above heights of 300–800 km. Below this layer, the particles responsible for the current are only weakly magnetized, i.e., they have a small ratio of cyclotron frequency over collision frequency. As a result the conductivity is isotropic, which prevents significant dissipation. The efficiency of dissipation drops steeply in the transition region because the field becomes increasingly force free, i.e., has no current component perpendicular to the field, explaining why the current sheet is not apparent in the *TRACE* data.

A sensible question would be whether we were able to observe the current sheet because of better spatial resolution, or whether special conditions lead to the presence of the current sheet at the time we observed it. The filamentary current structures found by Socas-Navarro (2005b) (without a clear concomitant heating signature) would indicate that these phenomena are more common in active regions. Indeed, the weakening of the current sheet observed on the next day would indicate that we caught the current sheet in an exceptionally bright phase.

We rely on potential field extrapolation from photospheric magnetograms to estimate the field configuration in the chromosphere. However, since the field is not force free (as evidenced by the presence of the current sheet), this is a procedure with limited validity. It would be preferable if the field could be measured directly in the chromosphere. Fortunately, IBIS has recently been upgraded to full Stokes capabilities, making precisely such measurements possible. With access to full Stokes polarimetry in chromospheric lines like the Ca II 854.2 nm, the detection and identification of current sheets like the one presented here, and the determination of their properties should vastly improve.

The authors thank Adriaan van Ballegooijen for providing the field extrapolation procedure.

REFERENCES

Bloomfield, D. S., Lagg, A., & Solanki, S. K. 2007, ApJ, 671, 1005
Carlsson, M., & Stein, R. F. 1997, ApJ, 481, 500
Cauzzi, G., et al. 2008, A&A, 480, 515
Cavallini, F. 2006, Sol. Phys., 236, 415
Demoulin, P., Henoux, J. C., Priest, E. R., & Mandrini, C. H. 1996, A&A, 308, 643
Goodman, M. L. 2004, A&A, 416, 1159
Handy, B. N., et al. 1999, Sol. Phys., 187, 229
Ji, H., Wang, H., Goode, P. R., Jiang, Y., & Yurchyshyn, V. 2004, ApJ, 607, L55
Jurcak, J., & Katsukawa, Y. 2008, A&A, 488, L33
Katsukawa, Y., et al. 2007, Science, 318, 1594
Parker, E. N. 1983a, ApJ, 264, 635
———. 1983b, ApJ, 264, 642
Priest, E. R. 1987, Solar Magnetohydrodynamics (Dordrecht: D. Reidel)
Priest, E. R., & Démoulin, P. 1995, J. Geophys. Res., 100, 23443
Reardon, K. P., & Cavallini, F. 2008, A&A, 481, 897
Rimmele, T. R. 2004, ApJ, 604, 906
Scherrer, P. H., Bogart, R. S., Bush, R. I., Hoeksema, J. T., Kosovichev, A. G., Schou, J., & MDI Engineering Team. 1995, Sol. Phys., 162, 129
Schmidt, W., Stix, M., & Wöhl, H. 1999, A&A, 346, 633
Socas-Navarro, H. 2005a, ApJ, 631, L167
———. 2005b, ApJ, 633, L57
Socas-Navarro, H., Trujillo Bueno, J., & Ruiz Cobo, B. 2000, ApJ, 530, 977
Solanki, S. K., Lagg, A., Woch, J., Krupp, N., & Collados, M. 2003, Nature, 425, 692
Uitenbroek, H. 2006, in ASP Conf. Ser. 354, Solar MHD Theory and Observations: A High Spatial Resolution Perspective, ed. J. Leibacher, R. F. Stein, & H. Uitenbroek (San Francisco: ASP), 313
Uitenbroek, H., Balasubramaniam, K. S., & Tritschler, A. 2006, ApJ, 645, 776